

# CD10/Nepriylsin Enrichment in Infrapatellar Fat Pad–Derived Mesenchymal Stem Cells Under Regulatory-Compliant Conditions

## Implications for Efficient Synovitis and Fat Pad Fibrosis Reversal

Dimitrios Kouroupis,<sup>\*†</sup> PhD, Annie C. Bowles,<sup>\*†‡</sup> PhD, Thomas M. Best,<sup>\* MD, PhD,</sup>  
Lee D. Kaplan,<sup>\* MD,</sup> and Diego Correa,<sup>\*†§ MD, MSc, PhD</sup>

*Investigation performed at the Department of Orthopedics, Miller School of Medicine, University of Miami, Miami, Florida, USA*

---

**Background:** Synovitis and infrapatellar fat pad (IFP) fibrosis participate in various conditions of the knee. Substance P (SP), a neurotransmitter secreted within those structures and historically associated with nociception, also modulates local neurogenic inflammatory and fibrotic responses. Exposure of IFP mesenchymal stem cells (IFP-MSCs) to a proinflammatory/profibrotic environment (ex vivo priming with TNF $\alpha$ , IFN $\gamma$ , and CTGF) induces their expression of CD10/nepriylsin, effectively degrading SP in vitro and in vivo.

**Purpose/Hypothesis:** The purpose was to test the therapeutic effects of IFP-MSCs processed under regulatory-compliant protocols, comparing them side-by-side with standard fetal bovine serum (FBS)–grown cells. The hypothesis was that when processed under such protocols, IFP-MSCs do not require ex vivo priming to acquire a CD10-rich phenotype efficiently degrading SP and reversing synovitis and IFP fibrosis.

**Study Design:** Controlled laboratory study.

**Methods:** Human IFP-MSCs were processed in FBS or either of 2 alternative conditions—regulatory-compliant pooled human platelet lysate (hPL) and chemically reinforced medium (Ch-R)—and then subjected to proinflammatory/profibrotic priming with TNF $\alpha$ , IFN $\gamma$ , and CTGF. Cells were assessed for in vitro proliferation, stemness, immunophenotype, differentiation potential, transcriptional and secretory profiles, and SP degradation. Based on a rat model of acute synovitis and IFP fibrosis, the in vivo efficacy of cells degrading SP plus reversing structural signs of inflammation and fibrosis was assessed.

**Results:** When compared with FBS, IFP-MSCs processed with either hPL or Ch-R exhibited a CD10<sup>High</sup> phenotype and showed enhanced proliferation, differentiation, and immunomodulatory transcriptional and secretory profiles (amplified by priming). Both methods recapitulated and augmented the secretion of growth factors seen with FBS plus priming, with some differences between them. Functionally, in vitro SP degradation was more efficient in hPL and Ch-R, confirmed upon intra-articular injection in vivo where CD10-rich IFP-MSCs also dramatically reversed signs of synovitis and IFP fibrosis even without priming or at significantly lower cell doses.

**Conclusion:** hPL and Ch-R formulations can effectively replace FBS plus priming to induce specific therapeutic attributes in IFP-MSCs. The resulting fine-tuned, regulatory-compliant, cell-based product has potential future utilization as a novel minimally invasive cell therapy for the treatment of synovitis and IFP fibrosis.

**Clinical Relevance:** The therapeutic enhancement of IFP-MSCs manufactured under regulatory-compliant conditions suggests that such a strategy could accelerate the time from preclinical to clinical phases. The therapeutic efficacy obtained at lower MSC numbers than currently needed and the avoidance of cell priming for efficient results could have a significant effect on the design of clinical protocols to potentially treat conditions involving synovitis and IFP fibrosis.

**Keywords:** mesenchymal stem cells (MSC); infrapatellar fat pad (IFP); CD10/nepriylsin; substance P; synovitis; IFP fibrosis; human platelet lysate (hPL); chemically reinforced media (Ch-R)

---

knee, including early-stage and progressive osteoarthritis<sup>2,16,18,33,40,44,45,47</sup> and arthrofibrotic lesions manifesting in anterior knee pain.<sup>15</sup> Both tissues serve as sites for immune cell infiltration with subsequent inflammation and fibrosis and as a source of proinflammatory molecules and joint destructive mediators, such as matrix metalloproteinases. These events are facilitated by the proinflammatory activities of mediators such as substance P (SP), which, in addition to its established roles in nociception, mediates neurogenic inflammation resulting from vasodilation and extravasation of immune cells within the IFP.<sup>4</sup>

Treating synovial and IFP inflammation and fibrosis at early stages could have an effect on the progression of such chronic conditions<sup>26</sup> by limiting the secretion of proinflammatory and catabolic molecules.<sup>2,16,18,33,36,40,45,47</sup> Mesenchymal stem cell (MSC)-based therapy has gained attention as a potential therapeutic alternative for inflammatory conditions, given their immunomodulatory and trophic effects involving anti-inflammatory and anti-fibrotic actions.<sup>9</sup> On this basis, we have shown that IFP-MSCs grown in “traditional” medium supplemented with fetal bovine serum (FBS) and exposed to a proinflammatory/profibrotic environment (ie, ex vivo priming with TNF $\alpha$ , IFN $\gamma$ , and CTGF) enhanced their immunomodulatory effects.<sup>29</sup> In parallel, ex vivo priming significantly induced a CD10-enriched IFP-MSC phenotype that effectively degraded SP in vitro and in vivo in a rat model of acute synovitis and IFP fibrosis. These findings invite the possibility of designing novel therapeutic strategies for patients with chronic conditions of the knee involving inflammation and fibrosis based on the control of SP presence and activity.

CD10, also known as neprilysin, is a surface neutral endopeptidase<sup>37</sup> expressed in multiple cells, including MSCs<sup>6,7,42</sup> and specifically IFP-MSCs.<sup>29</sup> The anti-inflammatory effects of CD10 have long been recognized in other systems,<sup>46,48</sup> while its presence in IFP-MSCs seems to be critical for efficient SP degradation, both in vitro and in vivo.<sup>29</sup> Therefore, phenotypic stability of the cells becomes a desired trait during the cell-based product manufacturing process. In the present study, we first compared phenotypic, molecular, and secretory profiles and the in vitro SP degradation potential of IFP-MSCs processed now under regulatory-compliant practices (human pooled platelet lysate [hPL]) and chemically reinforced medium (Ch-R) formulations. Second, we confirmed in vivo the SP degradation while assessing the therapeutic efficacy of the cells reversing synovitis and IFP fibrosis. The results following regulatory-compliant practices are side-by-side

contrasted with cells grown in standard FBS-containing media in an effort to provide strategies that could reduce the time between preclinical and clinical phases.

Safety concerns have been raised regarding the use of FBS-containing media during the manufacturing of MSC preparations for clinical applications, most of them related to prion exposure risk, toxicological risk, and immunological risk.<sup>19,41</sup> However, serial MSC expansion under these conditions to obtain clinically relevant therapeutic cell numbers may result in detrimental effects on cell performance (eg, compromised proliferation and/or accelerated senescence) or even untoward consequences to specific cell attributes (eg, phenotypic display and functional outcomes). These variable responses to processing steps, combined with the inherent interdonor variability, negatively affect the standardization and reproducibility of their therapeutic potential.

In the past decade, xeno-free formulations for MSC processing have become more popular as promising replacements for FBS. hPL and Ch-R are examples of such formulations. In a pioneering study, Doucet et al<sup>14</sup> proposed hPL as a potent source of bioactive molecules stored in platelet  $\alpha$ -granules for the ex vivo expansion of MSCs. Among the bioactive molecules are growth factors (GFs), including platelet-derived GF (PDGF), epidermal GF (EGF), insulin-like GF (IGF), transforming GF (TGF), and fibroblast GF 2.<sup>17,25</sup> Pilot clinical studies investigating the immunosuppressive effects of hPL-expanded MSCs in acute and chronic graft-versus-host disease observed no acute or late adverse effects at a median follow-up of 8 months, including patients receiving up to 5 MSC infusions.<sup>5,34</sup> Most important, Centeno et al<sup>10</sup> showed the applicability of autologous hPL-expanded MSC injections in the regeneration of meniscal lesions.

Herein, we describe how regulatory-compliant hPL and Ch-R enhanced proliferative responses, differentiation potential, and secretory and functional profiles and induced phenotypic adaptations in IFP-MSCs (ie, CD10 enrichment) directly related to consistently efficient SP degradation in vitro and in vivo. Furthermore, CD10 presence in IFP-MSCs resulted as being determinant to efficiently reverse synovitis and IFP fibrosis in vivo, even without previous ex vivo priming and at significantly lower cell doses. The incorporation of those manufacturing practices during the generation of IFP-MSC-based products could significantly affect the musculoskeletal cell therapy field in general, particularly conditions involving chronic inflammation and fibrosis, where targeted mechanistic therapies for early disease and its progression remain elusive.

<sup>§</sup>Address correspondence to Diego Correa, MD, MSc, PhD, Diabetes Research Institute and Cell Transplant Center, Miller School of Medicine, University of Miami, 1450 NW 10th Ave, Room 3014, Miami, FL 33136, USA (email: dxc821@med.miami.edu) (Twitter: DiegoCorreaMED).

\*Department of Orthopedics, UHealth Sports Medicine Institute, Miller School of Medicine, University of Miami, Miami, Florida, USA.

<sup>†</sup>Diabetes Research Institute and Cell Transplant Center, Miller School of Medicine, University of Miami, Miami, Florida, USA.

<sup>‡</sup>Department of Biomedical Engineering, College of Engineering, University of Miami, Miami, Florida, USA.

Submitted October 17, 2019; accepted February 19, 2020.

One or more of the authors has declared the following potential conflict of interest or source of funding: T.M.B. has received hospitality payments from GE Healthcare. L.D.K. has received hospitality and education payments from Arthrex and royalties or license fees from Smith & Nephew. AOSSM checks author disclosures against the Open Payments Database (OPD). AOSSM has not conducted an independent investigation on the OPD and disclaims any liability or responsibility relating thereto.

## METHODS

All materials and methods are thoroughly described in the Appendix Materials and Methods (available in the online version of the article).

### Isolation, Culture, and Expansion of IFP-MSCs

Following informed consent, IFP-MSCs were isolated from IFP tissue obtained from deidentified nonarthritic patients (n = 8; 2 male [16 and 26 years old] and 6 female [22, 26, 31, 44, 46, and 53 years old]) undergoing elective knee arthroscopy at the Lennar Foundation Medical Center, University of Miami. All procedures were carried out in accordance with relevant guidelines and regulations and following a protocol determined by the University of Miami Institutional Review Board not as human research (based on the nature of the samples as discarded tissue). Isolated IFP-MSCs were seeded in vitro and cultured in 3 complete media: hPL, Ch-R, and Dulbecco's modified Eagle medium (DMEM)–10% FBS.

### Clonogenic Assay

Passage 3 IFP-MSCs (n = 5) were seeded in 100-mm culture plates in duplicate at a density of 10<sup>3</sup> cells per plate in all 3 culturing conditions. On day 10, colony-forming unit fibroblasts (CFU-Fs) were manually enumerated after cytochemical staining with 0.01% crystal violet (Sigma).

### Cell Growth Kinetics Measurement

Passage 3 IFP-MSCs (n = 5) were seeded in 6-well plates at a density of 10<sup>4</sup> cells per well in all 3 culturing conditions. Growth curves were generated from bright-field images obtained with the IncuCyte Live Cell Analysis System with IncuCyte ZOOM software (Essen Bioscience) to quantify cell confluence as a percentage for a 10-day period.

### Proinflammatory/Profibrotic Priming With TNF $\alpha$ , IFN $\gamma$ , and CTGF

Passage 3 IFP-MSCs (n = 3) expanded in all 3 culturing conditions were subsequently primed with a proinflammatory/profibrotic cocktail (15 ng/mL, TNF $\alpha$ ; 10 ng/mL, IFN $\gamma$ ; 10 ng/mL CTGF; collectively called TIC) for 72 hours. Noninduced and TIC-induced cultures were evaluated for their phenotypic profiles by flow cytometric analysis.

### Immunophenotyping

Flow cytometric analysis was performed on passage 3–naïve and TIC-primed IFP-MSCs (n = 3) expanded in all 3 culturing conditions.

### Molecular Characterization

All samples (n = 3) were analyzed via selected human transcript primers (Appendix Table A1, available online) by quantitative polymerase chain reaction with QuantiFast

SYBR Green and a predesigned 28-gene TaqMan low-density cytokine array.

### Trilineage Differentiation

Osteogenic, chondrogenic, and adipogenic differentiation potential was evaluated in IFP-MSCs (n = 5) expanded in all 3 culturing conditions similar to previously published protocols.<sup>30</sup>

### Secretome Analysis

A protein array of 41 GFs was used to determine secreted levels obtained from IFP-MSCs (n = 2) expanded in all 3 culturing conditions with and without priming, and putative interactomes were generated by the STRING database (Search Tool for Retrieval of Interacting Genes/Proteins, v 11.0; <http://string-db.org>). Based on protein-protein interactions, the biological processes analyzed were related with regulation of (1) cell population proliferation (GO:0008284), (2) response to stimulus (GO:0048584), (3) cell migration (GO:0030335), (4) signal transduction (GO:0009966), (5) signaling receptor activity (GO:0010469), and (6) protein phosphorylation (GO:0006468). The KEGG interactome pathways analyzed were cytokine–cytokine receptor interaction (hsa04060), MAPK (hsa04010), PI3K-Akt (hsa04151), Ras (hsa04014), Jak-STAT (hsa04630), and Rap1 (hsa04015).

### SP In Vitro Assay

Parameter SP competitive immunoassay (R&D Systems) was used to quantify the levels (pg/mL) of endogenous and exogenously added SP to culture-expanded IFP-MSCs in all 3 culturing conditions (10<sup>5</sup> per well, 12 wells, n = 2 per culturing condition; “cells group”) and their derived supernatant without cells (“supernatant group”), following the manufacturer's instructions.

### CD10 Immunolocalization

IFP-MSC groups were fixed, washed with phosphate-buffered saline, incubated with anti-human CD10 polyclonal antibody (R&D Systems), and visualized with a Leica DMi8 microscope and Leica X software.

### CD10 Immunomagnetic Separation

Crude IFP-MSC preparations were immunomagnetically separated on the basis of CD10 expression through the Invitrogen CELLection Dynabeads Biotin Binder Kit (Thermo Fisher Scientific), according to manufacturer's instructions, resulting in CD10<sup>+</sup> and CD10<sup>−</sup> cohorts.

### Monoiodoacetate Model of Acute Synovitis and IFP Fibrosis

The animal protocol was approved by the institutional animal care and use committee of the University of Miami (16-

008-ad03) and conducted in accordance to the ARRIVE (Animal Research: Reporting of In Vivo Experiments) guidelines.<sup>27</sup> Sixteen 10-week-old Sprague-Dawley rats were used (8 males and 8 females; mean weight: 250 g and 200 g, respectively). The animals were housed to acclimate for 1 week before the experiment initiation. One rat was housed per cage in a sanitary ventilated room with controlled temperature and humidity and under a 12-/12-hour light/dark cycle with food and water provided ad libitum. Acute synovitis and IFP fibrosis were generated by intra-articular injection of 1 mg of monoiodoacetate in 50  $\mu$ L of saline in the right knee. Three days later, a single intra-articular injection of 500,000 or 50,000 cells in 50  $\mu$ L of Euro-Collins solution (MediaTech) was performed. To evaluate the therapeutic efficacy of IFP-MSCs with respect to their CD10 levels, different groups were used according to their positivity (Appendix Figure A1, available online):

*Lowest:* noninduced cells grown in FBS

*Intermediate:* immunomagnetically selected CD10<sup>-</sup>; re-expanded for 1 week in regulatory-compliant medium

*Highest:* immunomagnetically selected CD10<sup>+</sup>; noninduced, primed, and grown in regulatory-compliant medium

Animals were sacrificed 4 days after IFP-MSC injection (7 days total) for tissue harvesting and analysis.

## Histology

Rat knee joints were harvested by cutting the femur and tibia/fibula 1 cm above and below the joint line; muscles were removed; and joints were fixed with 10% neutral buffered formalin (Sigma-Aldrich) for 14 days at room temperature. Knee joints were decalcified, cut in half at the sagittal plane, and embedded in paraffin, and serial 4- $\mu$ m sections were obtained. Hematoxylin and eosin and Masson trichrome stainings were performed to evaluate the general morphology and degree of fibrosis of the synovium and IFP, respectively. The latter stain identifies collagen fiber-rich fibrotic areas (blue) and cells (pink cytoplasm and brown nucleus).

## SP Immunolocalization

Rat knee joints were harvested, fixed, and cut in half at the sagittal plane. Sections were incubated with anti-rat SP polyclonal antibody (Millipore) and visualized with a Leica DMi8 microscope and Leica X software.

## Statistical Analysis

Statistical analysis was performed with paired and unpaired Student *t* tests for normally distributed data and the Wilcoxon test (for paired data) or Mann-Whitney test (for unpaired data) in the presence of a nonnormal distribution; 1-way analysis of variance was used for multiple comparisons. All tests were performed with GraphPad

Prism (v 7.03; GraphPad Software). Level of significance was set at  $P < .05$ .

## Data Availability

All data generated or analyzed during this study are included in this published article (and Appendix, available online).

## RESULTS

### IFP-MSCs Show Superior Growth Kinetics When Expanded in Either hPL or Ch-R vs FBS

We first assessed the growth kinetics and clonogenic potential of IFP-MSCs expanded in either hPL or Ch-R and compared them with FBS alone. All 3 culture conditions demonstrated variable growth kinetics for 8 days. In detail, hPL-expanded IFP-MSCs showed an increased growth rate, reaching 85% confluency as compared with the FBS cultures, which had only 62% confluency on day 8. Ch-R medium showed the most potent growth rate versus the other 2 culturing conditions, entering confluency (>85%) only 4 days after seeding in vitro (Figure 1, A and B). However, clonogenic capacity showed a higher trend in FBS-expanded IFP-MSCs (mean  $\pm$  SD, 296  $\pm$  77 CFU-Fs) as compared with hPL and Ch-R (252  $\pm$  43 and 233  $\pm$  45 CFU-Fs, respectively) (Figure 1C).

### IFP-MSCs Expanded in Either hPL or Ch-R Have Privileged Immunophenotypic and Molecular Profiles

In all 3 culture conditions without TIC priming (ie, noninduced), the common MSC-defining markers (CD44, CD73, CD90, CD105, CD166) showed a similar expression pattern (>90% positivity), while LepR and CD56 were absent, and CD271 and CD200 had low to negative expression. NG2 showed high expression (approximately 90%) only in Ch-R (Figure 2A). Most important, markers related to MSC functionality toward an immunomodulatory and antifibrotic phenotype were significantly increased in noninduced IFP-MSCs by solely culturing in either hPL or Ch-R. In hPL-expanded IFP-MSCs, the mean expression of CD146 (44.1%  $\pm$  18.7%), CD10 (88.1%  $\pm$  6.2%), and CXCR4 (57.7%  $\pm$  17.01%) was 8-, 7-, and 5-fold enriched as compared with FBS medium cultures. Proinflammatory/profibrotic ex vivo priming with TIC for 72 hours resulted in CD146 and CD10 expression enrichment in all 3 culturing conditions (Figure 2B). IFP-MSCs expanded in hPL with TIC priming increased CD10 and CD146 expression by 1- and 1.6-fold, respectively. Even though CD10 expression increased by 1.8-fold in cultures with FBS plus TIC priming, these levels were still lower than in IFP-MSCs expanded in hPL without TIC priming (74.8  $\pm$  3.6% vs 88.9  $\pm$  4.1%). CD90 had stable expression (>90%) whereas, as expected and previously reported,<sup>11,21</sup> HLA-DR expression was sharply increased in all cultures with TIC priming.

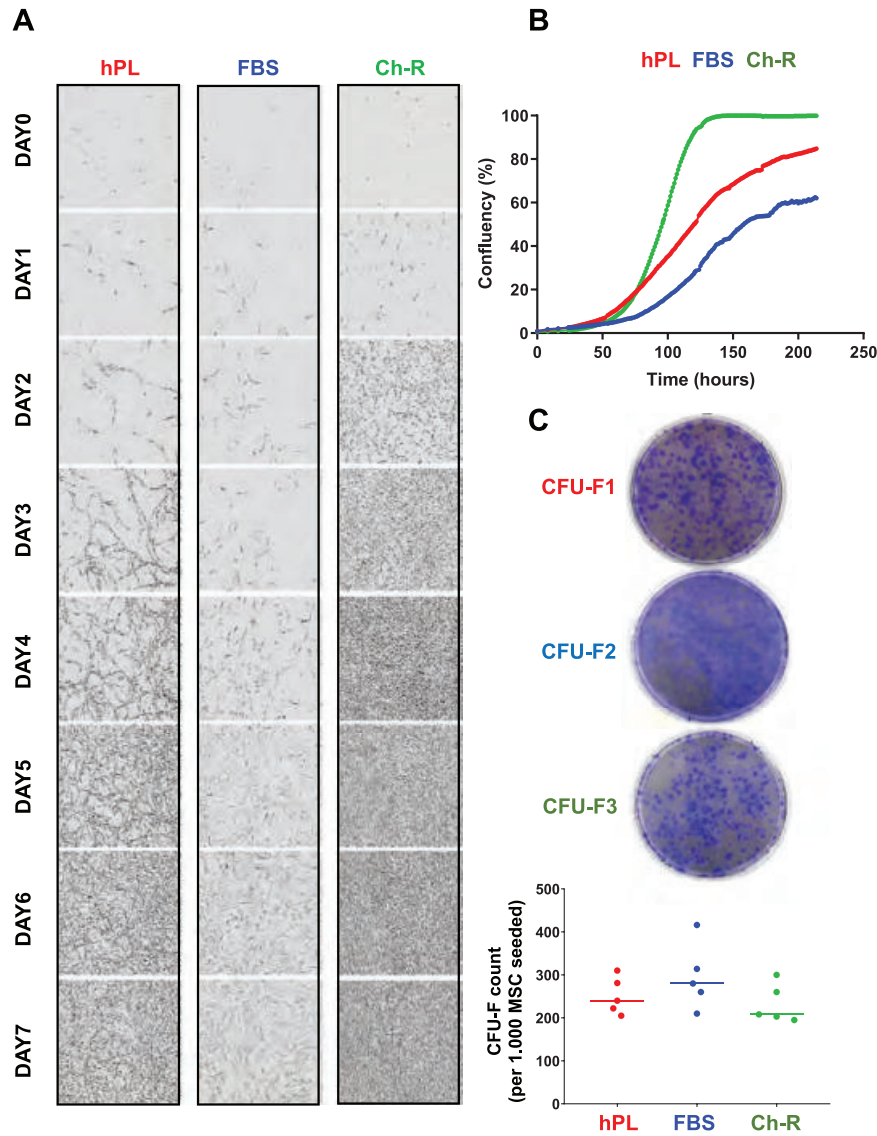


**Figure 1.** IFP-MSCs show high growth kinetics and clonogenicity when expanded in either hPL or Ch-R. (A, B) IFP-MSCs expanded in either hPL or Ch-R show a higher growth rate until confluency as compared with FBS alone. (C) Clonogenic capacity of FBS-expanded IFP-MSCs (colony-forming unit fibroblasts [CFU-Fs] per 10<sup>3</sup> MSCs seeded) showed a higher trend versus the other conditions. All experiments (n = 5) were performed independently, and data are presented as scatter plots with mean. Ch-R, chemically reinforced medium; FBS, fetal bovine serum; hPL, human platelet lysate; IFP, infrapatellar fat pad; MSC, mesenchymal stem cell.

### IFP-MSCs Expanded in Either hPL or Ch-R Can Effectively Differentiate Toward Bone, Fat, and Cartilage In Vitro

The tripotential capacity of IFP-MSCs to undergo osteogenic, chondrogenic, or adipogenic differentiation was comparable in FBS, hPL, and Ch-R. However, qualitative assessments showed that hPL- and Ch-R-expanded IFP-MSCs deposited higher levels of minerals on the monolayer surface in osteogenesis, had higher lipid vacuole accumulation within the cytoplasm in adipogenesis, and displayed stronger cartilage-specific metachromasia for glycosaminoglycans produced in chondrogenesis as compared with FBS-expanded IFP-MSCs (Figure 3A). Quantitatively at

the molecular level, hPL- and Ch-R-expanded IFP-MSCs showed significantly ( $P < .05$ ) higher expression levels for the osteogenic gene *OMD*, adipogenic gene *FABP4*, and chondrogenic genes *ACAN* and *COMP* as compared with FBS-expanded IFP-MSCs (Figure 3B), indicating their increased maturity during the different differentiation schemes.

### IFP-MSCs Expanded in Either hPL or Ch-R Have a Reduced Baseline Inflammatory Transcriptome vs FBS

To establish a baseline inflammation-related molecular signature for IFP-MSCs expanded in either hPL or Ch-R

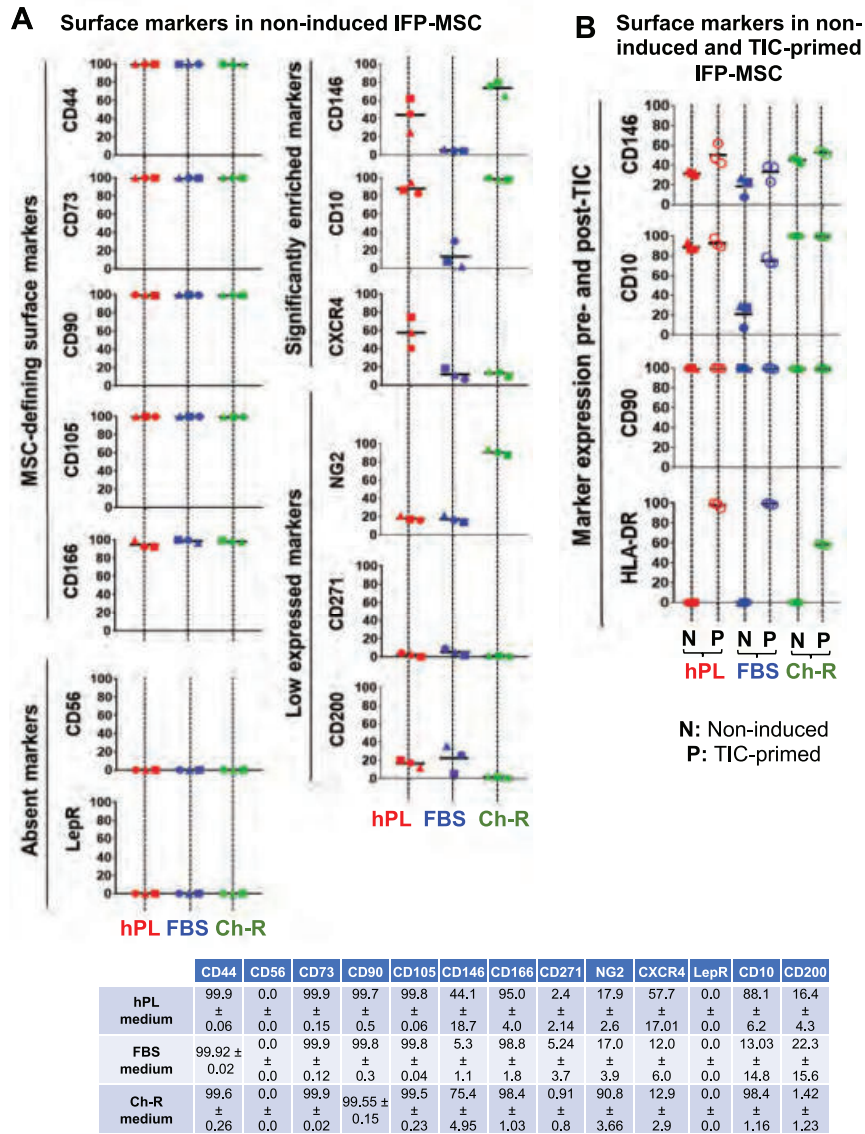


**Figure 2.** IFP-MSCs expanded in either hPL or Ch-R have enhanced immunophenotypic profile. (A) Surface markers assessed in noninduced IFP-MSCs show MSC-defining markers highly expressed in all culture conditions, whereas CD10 and CD146 (immunomodulatory) and CXCR4 (migratory) showed increased expression only in hPL and Ch-R. (B) Proinflammatory/profibrotic ex vivo priming with TNF $\alpha$ , IFN $\gamma$ , and CTGF (TIC) resulted in boosted expression of CD10 and CD146, while HLA-DR expression was induced as expected. All experiments (n = 3) were performed independently, and data are presented as scatter plots with mean. Individual donors in each MSC type are presented with distinctive shapes and color tones to allow intradonor comparisons. Ch-R, chemically reinforced medium; FBS, fetal bovine serum; hPL, human platelet lysate; IFP, infrapatellar fat pad; MSC, mesenchymal stem cell.

(noninduced), a multiplex transcriptional assessment was performed. IFP-MSCs grown in all 3 conditions showed an overall low-to-negative expression level for most inflammation-related cytokines tested (Figure 4A). Furthermore, when compared with FBS-grown cells, hPL- and Ch-R-expanded cells had reduced expression of most cytokines, with IL-18 significantly downregulated in both versus IL-1 $\beta$  and IL-12 $\alpha$  in only Ch-R (Figure 4B; Appendix Figure A2, available online). IL-8 was the only cytokine with significantly ( $P < .05$ ) higher expression levels in hPL- and Ch-R-expanded IFP-MSCs as compared with the FBS reference sample, with 6.8- and 8.6-fold

expression levels, respectively. Other molecules, such as IL-6, TNF- $\alpha$ , and IL-1 $\alpha$ , showed divergent changes with hPL and Ch-R.

### IFP-MSCs Expanded in Either hPL or Ch-R Strongly Secrete Reparative Factors Without Priming

Noninduced hPL-expanded IFP-MSCs showed overall higher secretion of GFs when compared with FBS medium (Figure 4B). Of the 41 GFs analyzed, 29 and 24 GFs were

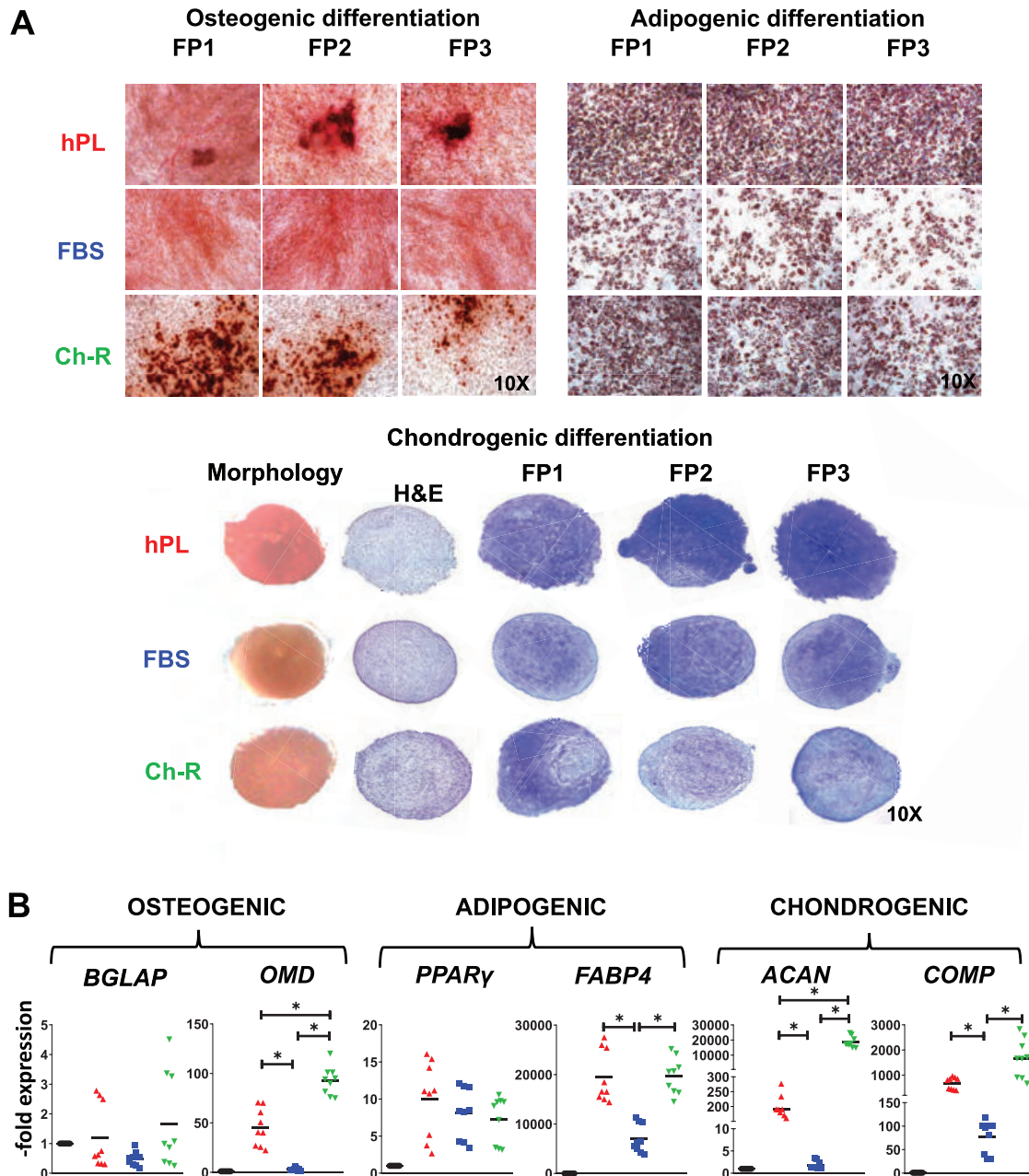


**Figure 3.** Osteogenic, chondrogenic, and adipogenic differentiation potential of IFP-MSC expanded in either hPL or Ch-R. (A) As compared with FBS-grown cells, hPL- and Ch-R-expanded IFP-MSCs showed superior qualitative differentiation capacity upon induction in vitro for bone (mineral deposition assessed by alizarin red staining), fat (lipid accumulation assessed by oil red staining), and cartilage (glycosaminoglycan production assessed by toluidine blue staining). (B) Quantitative molecular profiling showed that differentiation-related markers in cultures expanded in hPL and Ch-R were increased versus those expanded in FBS, indicating their mature status. All experiments (n = 5) were performed independently with noninduced cells, and data are presented as scatter plots with mean  $\pm$  SD. \* $P < .05$ . Ch-R, chemically reinforced medium; FBS, fetal bovine serum; H&E, hematoxylin and eosin; hPL, human platelet lysate; IFP, infrapatellar fat pad; MSC, mesenchymal stem cell.

secreted at significantly ( $P < .05$ ) higher levels in IFP-MSCs expanded in hPL and Ch-R without priming, respectively, as compared with FBS. Upon TIC priming, hPL- and Ch-R-expanded IFP-MSCs showed increased secretion of various proteins. However, the overall number of proteins secreted

was reduced, as TIC priming also affected the secretion of FBS-expanded IFP-MSCs. After TIC priming, 16 and 18 GFs were significantly ( $P < .05$ ) secreted higher in hPL- and Ch-R-expanded IFP-MSCs, respectively. Simultaneous Venn diagram representation of all 4 secretory profiles

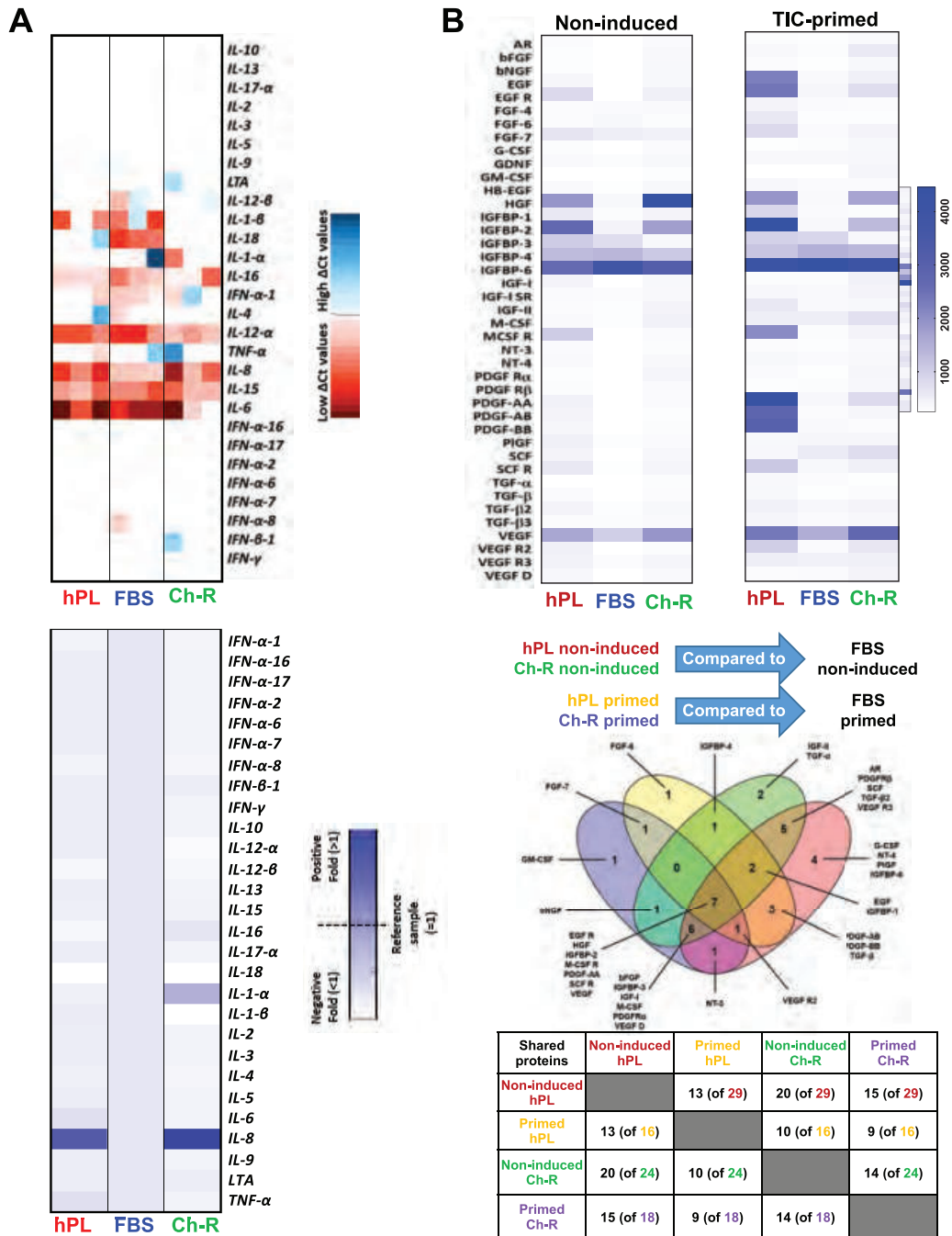


**Figure 4.** IFP-MSCs expanded in either hPL or Ch-R have a reduced inflammatory baseline signature while strongly secreting reparative growth factors. (A) Transcriptional profiling of IFP-MSCs expanded in all 3 formulations showed overall low-to-negative expression levels for most inflammation-related cytokines tested (top panel). This correlates with high delta Ct values in real-time quantitative polymerase chain reaction, representing the arithmetic subtraction of the Ct value of each gene minus the Ct value of the normalizing housekeeping gene and marked white to blue in the heat map. Lower panel shows the relative fold change expression (positive = darker, negative = lighter), calculated with the FBS-grown data as reference (set up as 1). For actual fold changes, see Appendix Figure A2 (available online). (B) Secretory profile heat maps of noninduced and TIC-primed IFP-MSCs indicated high growth factor secretion for hPL- and Ch-R-expanded IFP-MSCs (top panel). Heat maps colors are assigned according to a molecule concentration relative scale from 0 to 10,000. Venn diagram shows shared proteins among all groups (significantly different from FBS alone or FBS plus priming; middle panel). The table shows the number of proteins shared by different groups and conditions (lower panel). All experiments were performed independently (n = 3). Ch-R, chemically reinforced medium; FBS, fetal bovine serum; hPL, human platelet lysate; IFP, infrapatellar fat pad; MSC, mesenchymal stem cell; TIC, TNF $\alpha$ , IFN $\gamma$ , and CTGF.

(noninduced and primed hPL and noninduced and primed Ch-R), when compared with their FBS counterparts (noninduced and primed), revealed a core of 7 GFs (EGF R, HGF, IGFBP-2, M-CSF R, PDGF-AA, SCF R, VEGF) that are commonly increased in those 4 groups. Interestingly, after priming, 13 of 16 for hPL and 14 of 18 for Ch-R were shared with the secretory profiles in their noninduced state.

In protein association network analysis, GFs appeared interconnected at least through 1 association, while *K*-means clustering networks showed high protein-protein interaction enrichment ( $P < .0000000000000001$ ) and an average local clustering coefficient  $>0.7$ , indicating that the proteins used were at least partially biologically connected (Appendix Figure A3A, available online). In noninduced IFP-MSCs, hPL and Ch-R secretory profiles showed similar biological process involvement. Priming boosted the 5 of 6 biological processes of Ch-R-expanded IFP-MSCs versus only 3 of 6 in hPL-expanded IFP-MSCs (Appendix Figure A4A, left radar chart). The involvement in those biological processes was reflected in specific signaling pathways presented in the KEGG reactome (Appendix Figure A4A, right radar chart). In noninduced IFP-MSCs, hPL IFP-MSCs showed higher enrichment of the cytokine–cytokine receptor interaction and Jak-STAT (2 of 6) pathways, whereas Ch-R IFP-MSCs showed higher enrichment of the MAPK, PI3K-Akt, Ras, and Rap1 (4 of 6) pathways (Appendix Figure A4B). According to the KEGG database, the Jak-STAT pathway, which is highly enriched in hPL IFP-MSCs, is a principal downstream mechanism for an array of cytokines and GFs and is directly involved in cytokine–cytokine receptor interaction signaling (hsa:04060). Interestingly, in Ch-R IFP-MSCs—except the MAPK, PI3K-Akt, and Ras pathways, which are involved in downstream signaling upon cytokine and GF activation—the Rap1 pathway, which is involved in cell adhesion, cell-cell junction formation, and cell polarity, is also highly enriched. Most important, priming resulted in further-boosted protein involvement in all signaling pathways for both hPL- and Ch-R-primed IFP-MSCs.

### IFP-MSCs Expanded in Either hPL or Ch-R Secrete More Factors vs FBS Plus Priming

To assess the molecular similarities between the regulatory-compliant formulations and FBS plus priming, direct molecular comparisons were made between these groups. Secretory profile analysis revealed that noninduced hPL- and Ch-R-expanded IFP-MSCs shared with FBS plus priming 17 and 31 proteins, respectively. Importantly, except the common proteins shared, noninduced hPL IFP-MSCs showed a boosted secretory profile with 22 additional GFs highly secreted. In total, 14 proteins (AR, FGF-4, G-CSF, GDNF, GM-CSF, HB-EGF, IGFBP-4, IGF-I SR, IGF-II, NT-4, PDGFR $\beta$ , SCF, TGF- $\alpha$ , TGF- $\beta$ 3) were commonly and highly expressed in IFP-MSCs expanded in hPL and Ch-R (Figure 5). Overall, biological processes and interactome pathways analysis of the 3 groups compared (common noninduced hPL vs FBS plus priming, common noninduced Ch-R vs FBS plus priming,

common noninduced hPL vs noninduced Ch-R) showed similar protein involvement except few differences (Appendix Figure A4B, available online). Interestingly, group 1 showed a higher number of proteins involved in the “regulation of signaling receptor activity” process, whereas group 2 had a higher number of proteins involved in the “positive regulation of cell migration” process (Appendix Figure A4B, left radar chart). However, when compared with group 1, group 2 showed higher protein involvement in almost all KEGG reactome pathways tested except PI3K-Akt and Jak-STAT pathways (Appendix Figure A4B, right radar chart).

### IFP-MSCs Expanded in Either hPL or Ch-R Show Increased Functionality In Vitro

Upon exogenous addition of SP (834 pg/mL) in culture, the overall SP levels were significantly ( $P < .05$ ) decreased by the cell group and the supernatant group in all 3 conditions tested (Figure 6A). As compared with FBS, hPL and more so Ch-R induced a reduction of SP, statistically significant in the cells group but not in the supernatant group (for Ch-R). CD10 immunolocalization was detected in IFP-MSCs as a concentrated punctate signal around cells (Figure 6B), highly present in hPL- and Ch-R-expanded IFP-MSCs directly related to the SP degradation pattern observed after exogenous addition of SP in cultures. Importantly, 3-dimensional reconstruction of fibrinogen matrix formed in hPL cultures revealed that CD10<sup>+</sup> vesicles released from IFP-MSCs were immobilized within the 3-dimensional matrix (Figure 6C). This effect can be correlated with the limited capacity of hPL supernatants to degrade SP: an effect that was strongly induced by hPL-expanded IFP-MSCs.

### IFP-MSCs Expanded in Either hPL or Ch-R Effectively Reverse Synovitis and IFP Fibrosis and Degrade SP In Vivo

A rat model of induced acute synovitis and IFP fibrosis was used to confirm in vivo the degradation of SP and to test the capacity of IFP-MSCs with different levels of CD10 positivity to reverse synovial and IFP inflammation and fibrosis. In addition to signs of synovitis and early fibrotic changes of the IFP, we confirmed the hyperinnervation by SP-positive sensory fibers 7 days after the intra-articular injection of monoiodoacetate, as compared with healthy knees without inflammatory induction (Figure 7).

When compared with untreated animals, all animals that received IFP-MSCs showed a significant reduction in synovitis and IFP fibrosis 4 days after their administration (Figure 7, marked with arrows and asterisks, respectively). However, differences can be appreciated in the degree of inflammation and fibrosis reversal and SP degradation among animals that received IFP-MSCs with varying CD10 positivity, underscoring its relevance for an efficient therapeutic effect. Of note, and as support of the inductive CD10 enrichment with hPL and Ch-R, these

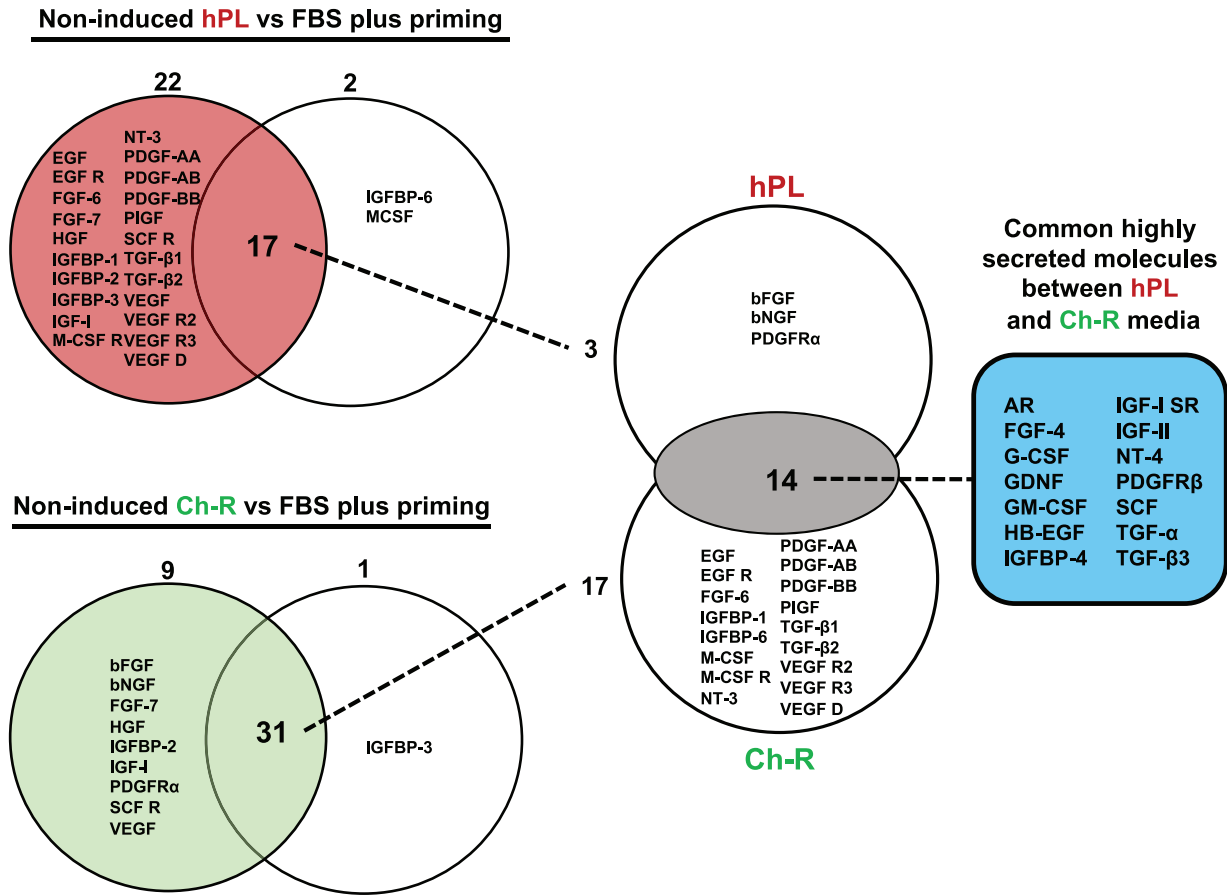


**Figure 5.** IFP-MSCs expanded in either hPL or Ch-R show high growth factor secretion when compared with FBS plus priming. Venn diagram analysis revealed shared proteins among the groups (significantly different from FBS plus priming), with 14 growth factors common and highly expressed in IFP-MSCs expanded in hPL and Ch-R. All experiments were performed independently (n = 2). Ch-R, chemically reinforced medium; FBS, fetal bovine serum; hPL, human platelet lysate; IFP, infrapatellar fat pad; MSC, mesenchymal stem cell.

formulations rapidly (1 week) turned the low CD10 positivity of immunomagnetically sorted CD10<sup>-</sup> IFP-MSCs (13 ± 14.8) into intermediate/high levels (74.6 ± 7.67) (Appendix Figure 1, available online). In our previous report, we clearly demonstrated the transient engraftment of injected IFP-MSCs in areas of active synovitis and IFP fibrosis.<sup>29</sup> In the present study, SP presence was also significantly diminished in rats after 4 days of single intra-articular injection of IFP-MSCs, being more pronounced in peripheral areas of the IFP (close to the synovium), whereas inner parts (IFP body) showed some remaining SP-positive fibers (Figure 7). This SP degradation was uniform across animals that received IFP-MSCs with high levels of CD10, while the ones that received IFP-MSCs with lower CD10 positivity (IFP-MSCs expanded in FBS) clearly showed suboptimal SP degradation. Of note, CD10<sup>+</sup>-selected IFP-MSCs showed the strongest reduction of synovitis and IFP fibrosis and SP degradation, while a reduction in the cell dose in 1 of 10 (total of 50,000 cells) still effectively generated therapeutic efficacy, as they were high in CD10 owing to the priming stimulation.

**DISCUSSION**

Synovitis and fibrosis of the IFP constitute early structural changes preceding the onset of osteoarthritis<sup>12,22-24,36</sup> while actively participating in other chronic conditions of the knee, including anterior knee pain<sup>15</sup> and even patellar tendinopathy, as suggested in animal models.<sup>28</sup> Inside synovium and IFP, the neuropeptide SP stands out for its multiple roles in the disease. In addition to established roles in nociception,<sup>32,52</sup> it participates in the modulation of local neurogenic inflammatory and immune responses.<sup>38,51</sup> SP activity is regulated in part by the cell membrane-bound neutral endopeptidase CD10/nepilysin (reviewed by Maguer-Satta et al<sup>37</sup>), expressed in multiple cells, including MSCs<sup>6,7,42</sup> and specifically IFP-MSCs as we recently reported.<sup>29</sup> In that study, we also demonstrated that IFP-MSCs cultured in FBS-containing medium and stimulated (ie, primed) with proinflammatory/profibrotic molecules (TIC) resulted in increased CD10 expression inducing the degradation of SP both in vitro and in vivo while showing strong immunomodulatory effects.<sup>29</sup>

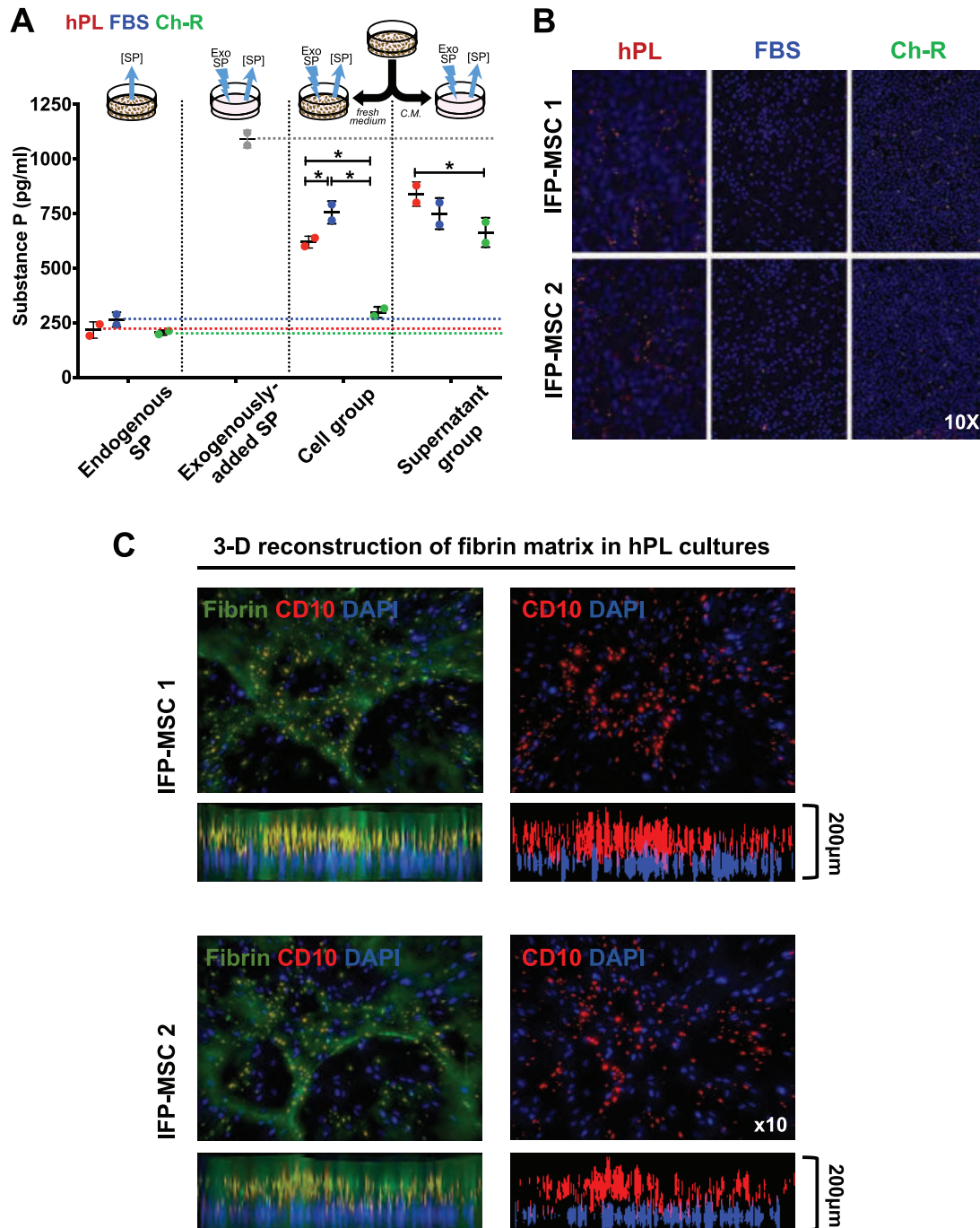


**Figure 6.** IFP-MSCs expanded in either hPL or Ch-R effectively degrade substance P (SP) in vitro. (A) Endogenous levels of SP (quantified at ~250 pg/mL and shown as dotted colored lines) and exogenously added recombinant SP (quantified at ~1100 pg/mL and shown as a gray dotted line) are used for reference (as bottom and top boundaries, respectively) to quantify SP degradation activity by the cells and their supernatant in the different media formulations. When compared with FBS-grown cells, hPL- and Ch-R-expanded IFP-MSCs (cell group) strongly degraded SP, an effect also present with their supernatant (less pronounced, though). A diagram on the top of each group represents the source of the samples obtained for the measurements. CM, conditioned media; Exo SP, exogenously added SP; [SP] = SP concentration. (B) CD10 immunolocalization was detected in IFP-MSCs as a concentrated punctate signal (red) around cells and highly present in hPL- and Ch-R-expanded IFP-MSCs (blue nuclei). (C) Fibrinogen matrix (green) formed within hPL cultures immobilized CD10<sup>+</sup> vesicles (red) released from IFP-MSCs (blue nuclei). All experiments were performed independently (n = 2), and data are presented as scatter plots with mean ± SD. \*P < .05. Ch-R, chemically reinforced medium; FBS, fetal bovine serum; hPL, human platelet lysate; IFP, infrapatellar fat pad; MSC, mesenchymal stem cell.

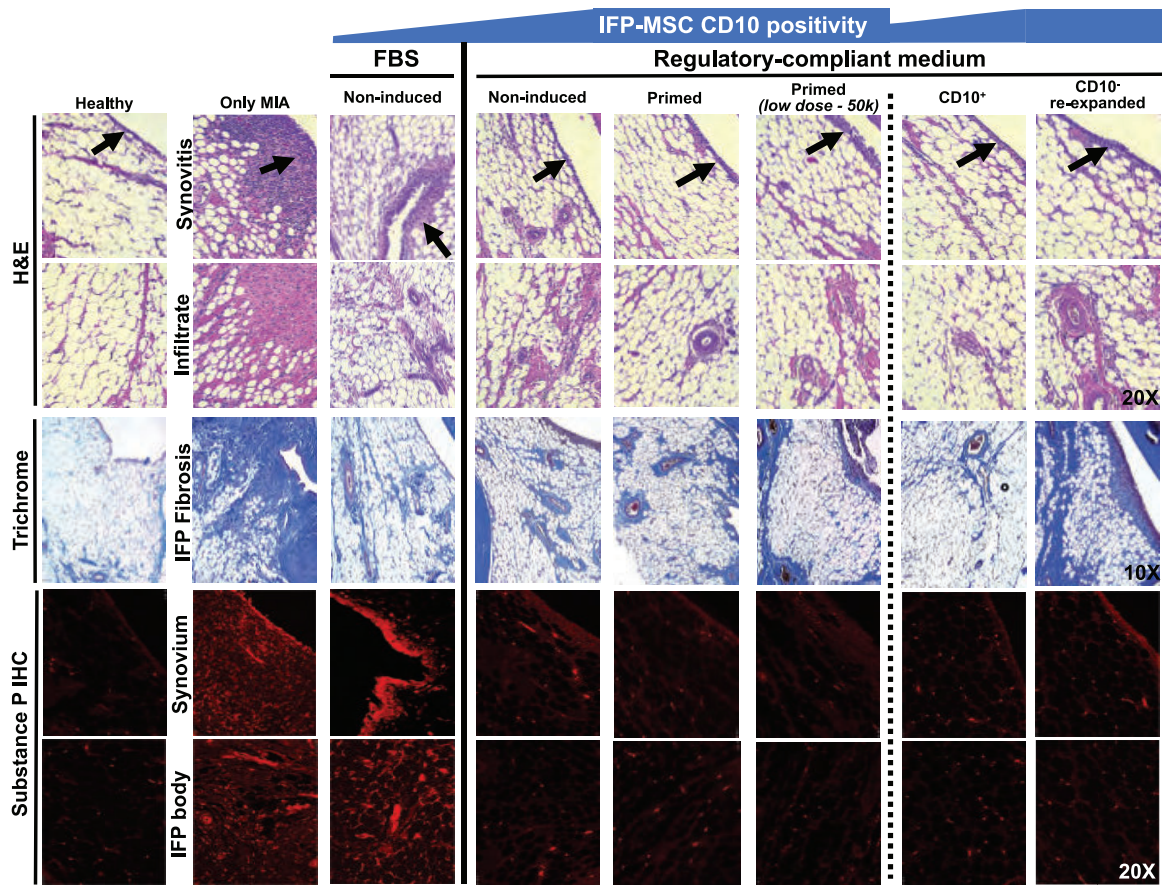


**Figure 7.** IFP-MSCs expanded in either hPL or Ch-R effectively reduce synovitis and IFP fibrosis in vivo. Hematoxylin and eosin (H&E) staining (top 2 panels), Masson trichrome staining (middle panel), and substance P immunolocalization (lower 2 panels) in sagittally sectioned knees of representative rats for healthy control and those injected with only MIA or both MIA and IFP-MSCs with different degrees of CD10 positivity. When compared with the MIA-only group, which showed significant synovitis and IFP fibrosis with cellular infiltrates, a striking correlation was found between magnitude of CD10 presence in IFP-MSCs and the effect of reducing those structural changes after 4 days of a single intra-articular IFP-MSC injection. Despite an overall significant reduction in synovitis and IFP fibrosis with all treatments, the immunoselected CD10<sup>+</sup> group expanded in regulatory-compliant medium showed the strongest therapeutic effect, whereas the CD10<sup>-</sup> re-expanded and noninduced FBS group had the poorest outcomes. The other groups (noninduced and primed IFP-MSCs expanded in regulatory-compliant medium) were effective, even at a lower dose (1/10th). SP<sup>+</sup> fibers in areas of active inflammation and fibrosis showed dramatic reduction for the synovium and the body of the IFP in groups similarly correlated with the degree of CD10 positivity. Of note, almost no signal was detected in healthy control rats, supporting the high specificity of the SP signal. Arrows in the top panel indicate areas of synovitis. Ch-R, chemically reinforced medium; FBS, fetal bovine serum; hPL, human platelet lysate; IFP, infrapatellar fat pad; IHC, immunohistochemistry; MIA, monoiodoacetate; MSC, mesenchymal stem cell; SP, substance P.

To build on our previous results, the present study aimed at investigating the therapeutic potential of IFP-MSCs in acute synovitis and IFP fibrosis, contrasting cell products manufactured with either regulatory-compliant or FBS-containing (DMEM–10% FBS) media, and with and without ex vivo inflammatory priming. Overall, we found that processing IFP-MSCs in either hPL or Ch-R results in enhanced proliferative response, differentiation potential, transcriptional and secretory profiles, and a significant intrinsic enrichment in CD10 and other key markers (CD146 and CXCR4). Functionally, these formulations induced IFP-MSCs to more efficiently degrade SP in vitro and in vivo and to efficiently reverse signs of

synovitis and IFP fibrosis even at lower cell doses, as explained by more robust and consistent CD10 expression. Molecularly, they recapitulated and enhanced the secretory panel of GFs and cytokines observed with FBS plus priming, thus replacing “traditional” FBS as a medium supplement and obviating the need of ex vivo priming to generate such enhanced therapeutic effects.

IFP-MSCs grown in FBS-containing medium exhibited a phenotype comparable with our previous findings.<sup>29</sup> In that report, we highlighted the importance of CD10 and CD146 expression levels as part of an immunomodulatory MSC functionality. Herein, we demonstrated that hPL and Ch-R formulations result in a significant ( $P < .05$ )

enrichment in both markers (8- and 7-fold, respectively), comparable with the levels obtained with primed cells in FBS, suggesting that the “desired” phenotype can be achieved without external inflammatory stimulation as long as they are processed in such xeno-free formulations. Upon exposure to TIC priming stimulation, which mimics inflammatory and fibrotic microenvironments,<sup>44,47</sup> CD146 expression increased under all 3 conditions. Priming also increased CD10 presence only in FBS-grown cells, indicating that the high levels induced by hPL and Ch-R formulations before priming had already reached maximum expression (close to 90%-95%). However, and relevant for clinical protocols, HLA-DR remained negative in IFP-MSCs grown in hPL and Ch-R, evidencing their immunoevasive phenotype. This was complemented by investigation of the inflammatory signature of the cells at the transcriptional level. For almost all inflammation-related cytokines tested, hPL- and Ch-R-expanded IFP-MSCs showed absent or very low gene expression levels. Despite comparable IL-6 expression levels across formulations, IL-8 was greater in regulatory-compliant media, making the IL-6/IL-8 ratio, previously identified as beneficial when low,<sup>1,29</sup> significantly lower in those conditions.

In terms of differentiation potential, IFP-MSCs processed in hPL and Ch-R enhanced differentiation toward the 3 MSC-related lineages proposed by the International Society for Cellular Therapy,<sup>13</sup> most notably in chondrogenesis. This complements our previous findings in which IFP-MSCs exhibit a stronger chondrogenic differentiation than bone marrow-derived MSCs.<sup>29</sup> Furthermore, a previous study showed that IFP-MSCs can not only effectively differentiate toward chondrocytes but also possess the capacity to secrete the superficial zone protein lubricin, which plays a crucial role in articular cartilage lubrication and normal function.<sup>31</sup>

The overall secretory response upon expansion in hPL or Ch-R involves the boosted secretion of a wide spectrum of immunomodulatory/repairatory GFs, including EGF, FGF, PDGF, HGF, TGF, SCF, VEGF, IGF-1, M-CSF, and AR. Physiologically, all these molecules are actively released in the in vivo microenvironment upon inflammatory stimulation and orchestrate the tissue regeneration process by inhibiting leukocyte transmigration, enhancing angiogenesis, increasing progenitor cell migration and differentiation, and modulating local macrophage responses.<sup>35</sup> In terms of biological processes, various categories were reinforced in hPL- or Ch-R-expanded IFP-MSCs, including cell proliferation, response to stimulus, cell migration, protein phosphorylation, signal transduction, and signaling receptor activity. Combined, these effects empower the cells to respond to inflammation and injury by increasing their numbers and migratory behavior to active sites of injury, while altering key cascades known to affect local immune responses.

CD10-mediated SP degradation in vitro was evident in all 3 culturing conditions, with differences in the efficiency that reflect the CD10 levels in the cells. Accordingly, high CD10 expression in hPL- and Ch-R-grown cells correlate with an observed increased SP degradation. Consistent with our previous report, supernatants obtained from the

same IFP-MSC cultures mimic (with varying degrees) the SP-degrading activities observed with their parental cells, suggesting that the mechanism used by IFP-MSCs to degrade SP is not necessarily cell bound but also released. A special case is the “suboptimal” results with hPL supernatant as compared with the other formulations, as explained by the active entrapment of the CD10<sup>+</sup> IFP-MSCs (and released CD10) within the fibrinogen-rich extracellular matrix of the hPL.

A striking correlation was found in our in vivo rat model studies between CD10 expression magnitude in IFP-MSCs and the reduction or even absence of SP<sup>+</sup> fibers in areas of active inflammation and fibrosis for the synovium and the body of the IFP. Similarly, they generated varying degrees of synovitis and IFP fibrosis reversal, having significant therapeutic implications. Based on the correlation between CD10 positivity and therapeutic outcome, levels around ≤30% have reduced effects, while levels ~70% or more “guarantee” an effective therapeutic outcome. The latter is based on the fact that all groups with CD10 levels beyond ~70% positivity exhibited comparable outcomes. Additional experimentation would be required to assess levels between 30% and 70% to establish a definitive threshold. Furthermore, the results obtained with the significantly reduced cell dose (1/10th of the injected cells) reinforce the concept of CD10 positivity rather than the number of cells injected as the pivotal factor for the generation of efficient therapeutic outcomes. Translated into a potential clinical protocol, this would reduce the required number of IFP-MSCs injected into numbers that can be generated in vitro in a shorter period. Based on the current standard of ~20 to 50 × 10<sup>6</sup> MSCs<sup>39,43,49</sup> for an intra-articular injection, the resulting protocol would require only ~2 to 5 × 10<sup>6</sup>. These effects are of utmost importance, as they suggest not only the possibility of reducing the manufacturing processing time to obtain clinically relevant cell numbers but also the elimination of the ex vivo inflammatory cell priming, which involves potential in vivo untoward consequences (eg, immunogenicity<sup>11,21</sup>). Taken together, these in vivo results suggest that IFP-MSCs exhibiting specific attributes at a certain level (CD10<sup>High</sup>) result in an attractive alternative to effectively treat synovitis and IFP fibrosis.

Clinical translation of cell-based therapies requires regulatory-compliant practices during the fabrication of the cellular product. On this basis, efforts are concentrated on defining protocols with minimal manipulation for the generation of clinically relevant cell numbers. To date, FBS-containing media have been widely used during MSC production for clinical trials, despite the reported risks and potential complications.<sup>50</sup> Consequently, cellular product manufacturing is migrating toward the use of xeno-free and chemically reinforced formulations (eg, hPL and Ch-R) to support MSC viability and proliferation and to preserve or even boost specific characteristics (eg, phenotype) and functional attributes.<sup>3,20</sup> In that respect, previous studies have shown that hPL contains a series of bioactive molecules (reviewed by Burnouf et al<sup>5</sup>) that can induce MSCs to acquire an immunomodulatory phenotype, potentially obviating the use of ex vivo cell priming. Our high-content in

vitro and in vivo data support these findings, specifically in the context of SP degradation and reversal of signs of synovitis and IFP fibrosis.

In conclusion, the use of hPL and Ch-R results in a fine-tuned, regulatory-compliant IFP-MSC cell-based product with enhanced growth kinetics, differentiation capacity, and an immunomodulatory secretory and phenotypic profile, with strong CD10-mediated SP degradation. From a therapeutic perspective, the local activities of injected IFP-MSCs relate with the control of (1) local inflammation and fibrosis of the synovium and IFP and (2) pain-related signaling via SP degradation. The retention and enhancement of IFP-MSC therapeutic properties, when manufactured under regulatory-compliant conditions, suggest that such an enhanced strategy could accelerate the time between preclinical and clinical research steps. This would facilitate the translation of proof-of-concept data into clinical protocols to treat synovitis and IFP fibrosis and potentially mitigate the progression of chronic conditions in which these processes participate.

## ACKNOWLEDGMENT

The authors thank Dylan Greif and Jared Gould for their contributions to this study. The authors are in gratitude with the Soffer Family Foundation and the DRI Foundation for their generous funding support. These funding sources were not involved in any step of the study design; collection, analysis, or interpretation of the data; or writing of the manuscript.

## REFERENCES

- Barajas-Gómez BA, Rosas-Carrasco O, Morales-Rosales SL, et al. Relationship of inflammatory profile of elderly patients serum and senescence-associated secretory phenotype with human breast cancer cells proliferation: role of IL6/IL8 ratio. *Cytokine*. 2017;91:13-29.
- Benito MJ, Veale DJ, FitzGerald O, van den Berg WB, Bresnihan B. Synovial tissue inflammation in early and late osteoarthritis. *Ann Rheum Dis*. 2005;64(9):1263-1267.
- Bobis-Wozowicz S, Kmiotek K, Kania K, et al. Diverse impact of xeno-free conditions on biological and regenerative properties of hUC-MSCs and their extracellular vesicles. *J Mol Med*. 2017;95(2):205-220.
- Bohnsack M, Meier F, Walter GF, et al. Distribution of substance-P nerves inside the infrapatellar fat pad and the adjacent synovial tissue: a neurohistological approach to anterior knee pain syndrome. *Arch Orthop Trauma Surg*. 2005;125(9):592-597.
- Bonin von M, Stölzel F, Goedecke A, et al. Treatment of refractory acute GVHD with third-party MSC expanded in platelet lysate-containing medium. *Bone Marrow Transplant*. 2009;43(3):245-251.
- Bourin P, Bunnell BA, Casteilla L, et al. Stromal cells from the adipose tissue-derived stromal vascular fraction and culture expanded adipose tissue-derived stromal/stem cells: a joint statement of the International Federation for Adipose Therapeutics and Science (IFATS) and the International Society for Cellular Therapy (ISCT). *Cytotherapy*. 2013;15(6):641-648.
- Buhring H-J, Tremel S, Cerabona F, de Zwart P, Kanz L, Sobiesiak M. Phenotypic characterization of distinct human bone marrow-derived MSC subsets. *Ann N Y Acad Sci*. 2009;1176(1):124-134.
- Burnouf T, Strunk D, Koh MBC, Schallmoser K. Human platelet lysate: replacing fetal bovine serum as a gold standard for human cell propagation? *Biomaterials*. 2016;76:371-387.
- Caplan AI, Correa D. The MSC: an injury drugstore. *Cell Stem Cell*. 2011;9(1):11-15.
- Centeno CJ, Busse D, Kisiday J, Keohan C, Freeman M, Karli D. Regeneration of meniscus cartilage in a knee treated with percutaneously implanted autologous mesenchymal stem cells. *Med Hypotheses*. 2008;71(6):900-908.
- Chan WK, Lau AS-Y, Li JC-B, Law HK-W, Lau YL, Chan GC-F. MHC expression kinetics and immunogenicity of mesenchymal stromal cells after short-term IFN-gamma challenge. *Exp Hematol*. 2008;36(11):1545-1555.
- Clockaerts S, Bastiaansen-Jenniskens YM, Runhaar J, et al. The infrapatellar fat pad should be considered as an active osteoarthritic joint tissue: a narrative review. *Osteoarthritis Cartilage*. 2010;18(7):876-882.
- Dominici M, Le Blanc K, Mueller I, et al. Minimal criteria for defining multipotent mesenchymal stromal cells: the International Society for Cellular Therapy position statement. *Cytotherapy*. 2006;8(4):315-317.
- Doucet C, Ernou I, Zhang Y, et al. Platelet lysates promote mesenchymal stem cell expansion: a safety substitute for animal serum in cell-based therapy applications. *J Cell Physiol*. 2005;205(2):228-236.
- Dragoo JL, Johnson C, McConnell J. Evaluation and treatment of disorders of the infrapatellar fat pad. *Sports Med*. 2012;42(1):51-67.
- Favero M, El-Hadi H, Belluzzi E, et al. Infrapatellar fat pad features in osteoarthritis: a histopathological and molecular study. *Rheumatology (Oxford)*. 2017;56(10):1784-1793.
- Fekete N, Gadelorge M, Fürst D, et al. Platelet lysate from whole blood-derived pooled platelet concentrates and apheresis-derived platelet concentrates for the isolation and expansion of human bone marrow mesenchymal stromal cells: production process, content and identification of active components. *Cytotherapy*. 2012;14(5):540-554.
- Felson DT, Niu J, Neogi T, et al. Synovitis and the risk of knee osteoarthritis: the MOST Study. *Osteoarthritis Cartilage*. 2016;24(3):458-464.
- Friedner OM, Allickson JG, Zhang N, et al. A consensus introduction to serum replacements and serum-free media for cellular therapies. *Cytotherapy*. 2017;19(2):155-169.
- Gerby S, Attebi E, Vlaski M, Ivanovic Z. A new clinical-scale serum-free xeno-free medium efficient in ex vivo amplification of mesenchymal stromal cells does not support mesenchymal stem cells. *Transfusion*. 2017;57(2):433-439.
- Griffin MD, Ryan AE, Alagesan S, Lohan P, Treacy O, Ritter T. Anti-donor immune responses elicited by allogeneic mesenchymal stem cells: what have we learned so far? *Immunol Cell Biol*. 2013;91(1):40-51.
- Harkey MS, Davis JE, Lu B, et al. Early pre-radiographic structural pathology precedes the onset of accelerated knee osteoarthritis. *BMC Musculoskelet Disord*. 2019;20(1):241.
- Ioan-Facsinay A, Kloppenburg M. An emerging player in knee osteoarthritis: the infrapatellar fat pad. *Arthritis Res Ther*. 2013;15(6):225.
- Jiang LF, Fang JH, Wu LD. Role of infrapatellar fat pad in pathological process of knee osteoarthritis: future applications in treatment. *WJCC*. 2019;7(16):2134-2142.
- Jung S, Sen A, Rosenberg L, Behie LA. Identification of growth and attachment factors for the serum-free isolation and expansion of human mesenchymal stromal cells. *Cytotherapy*. 2010;12(5):637-657.
- Kerna I, Kisand K, Suutres S, et al. The ADAM12 is upregulated in synovitis and postinflammatory fibrosis of the synovial membrane in patients with early radiographic osteoarthritis. *Joint Bone Spine*. 2014;81(1):51-56.
- Kilkenny C, Browne WJ, Cuthill IC, Emerson M, Altman DG. Improving bioscience research reporting: the ARRIVE guidelines for reporting animal research. *Osteoarthritis Cartilage*. 2012;20(4):256-260.

28. Kitagawa T, Nakase J, Takata Y, Shimosaki K, Asai K, Tsuchiya H. Histopathological study of the infrapatellar fat pad in the rat model of patellar tendinopathy: a basic study. *Knee*. 2019;26(1):14-19.
29. Kouroupis D, Bowles AC, Willman MA, et al. Infrapatellar fat pad-derived MSC response to inflammation and fibrosis induces an immunomodulatory phenotype involving CD10-mediated substance P degradation. *Sci Rep*. 2019;9(1):10864.
30. Kouroupis D, Kyrkou A, Triantafyllidi E, et al. Generation of stem cell-based bioartificial anterior cruciate ligament (ACL) grafts for effective ACL rupture repair. *Stem Cell Res*. 2016;17(2):448-457.
31. Lee SY, Nakagawa T, Reddi AH. Mesenchymal progenitor cells derived from synovium and infrapatellar fat pad as a source for superficial zone cartilage tissue engineering: analysis of superficial zone protein/lubricin expression. *Tissue Eng Part A*. 2010;16(1):317-325.
32. Lehner B, Koeck FX, Capellino S, Schubert TEO, Hofbauer R, Straub RH. Preponderance of sensory versus sympathetic nerve fibers and increased cellularity in the infrapatellar fat pad in anterior knee pain patients after primary arthroplasty. *J Orthop Res*. 2008;26(3):342-350.
33. Lieberthal J, Sambamurthy N, Scanzello CR. Inflammation in joint injury and post-traumatic osteoarthritis. *Osteoarthritis Cartilage*. 2015;23(11):1825-1834.
34. Lucchini G, Inrona M, Dander E, et al. Platelet-lysate-expanded mesenchymal stromal cells as a salvage therapy for severe resistant graft-versus-host disease in a pediatric population. *Biol Blood Marrow Transplant*. 2010;16(9):1293-1301.
35. Ma S, Xie N, Li W, Yuan B, Shi Y, Wang Y. Immunobiology of mesenchymal stem cells. *Cell Death Differ*. 2014;21(2):216-225.
36. Macchi V, Stocco E, Stecco C, et al. The infrapatellar fat pad and the synovial membrane: an anatomic-functional unit. *J Anat*. 2018;233(2):146-154.
37. Maguer-Satta V, Besançon R, Bachelard-Cascales E. Concise review: neutral endopeptidase (CD10): a multifaceted environment actor in stem cells, physiological mechanisms, and cancer. *Stem Cells*. 2011;29(3):389-396.
38. Mashaghi A, Marmalidou A, Tehrani M, Grace PM, Pothoulakis C, Dana R. Neuropeptide substance P and the immune response. *Cell Mol Life Sci*. 2016;73(22):4249-4264.
39. Matas J, Orrego M, Amenabar D, et al. Umbilical cord-derived mesenchymal stromal cells (MSCs) for knee osteoarthritis: repeated MSC dosing is superior to a single MSC dose and to hyaluronic acid in a controlled randomized phase I/II trial. *Stem Cells Transl Med*. 2019;8(3):215-224.
40. Mathiessen A, Conaghan PG. Synovitis in osteoarthritis: current understanding with therapeutic implications. *Arthritis Res Ther*. 2017;19(1):18.
41. Mendicino M, Bailey AM, Wonnacott K, Puri RK, Bauer SR. MSC-based product characterization for clinical trials: an FDA perspective. *Cell Stem Cell*. 2014;14(2):141-145.
42. Ong WK, Tan CS, Chan KL, et al. Identification of specific cell-surface markers of adipose-derived stem cells from subcutaneous and visceral fat depots. *Stem Cell Reports*. 2014;2(2):171-179.
43. Pers Y-M, Rackwitz L, Ferreira R, et al. Adipose mesenchymal stromal cell-based therapy for severe osteoarthritis of the knee: a phase I dose-escalation trial. *Stem Cells Transl Med*. 2016;5(7):847-856.
44. Remst DFG, Blaney Davidson EN, van der Kraan PM. Unravelling osteoarthritis-related synovial fibrosis: a step closer to solving joint stiffness. *Rheumatology (Oxford)*. 2015;54(11):1954-1963.
45. Scanzello CR, Goldring SR. The role of synovitis in osteoarthritis pathogenesis. *Bone*. 2012;51(2):249-257.
46. Shipp MA, Stefano GB, Switzer SN, Griffin JD, Reinherz EL. CD10 (CALLA)/neutral endopeptidase 24.11 modulates inflammatory peptide-induced changes in neutrophil morphology, migration, and adhesion proteins and is itself regulated by neutrophil activation. *Blood*. 1991;78(7):1834-1841.
47. Sokolove J, Lepus CM. Role of inflammation in the pathogenesis of osteoarthritis: latest findings and interpretations. *Ther Adv Musculoskelet Dis*. 2013;5(2):77-94.
48. Solan NJ, Ward PE, Sanders SP, Towns MC, Bathon JM. Soluble recombinant neutral endopeptidase (CD10) as a potential antiinflammatory agent. *Inflammation*. 1998;22(1):107-121.
49. Soler R, Orozco L, Munar A, et al. Final results of a phase I-II trial using ex vivo expanded autologous mesenchymal stromal cells for the treatment of osteoarthritis of the knee confirming safety and suggesting cartilage regeneration. *Knee*. 2016;23(4):647-654.
50. Spees JL, Gregory CA, Singh H, et al. Internalized antigens must be removed to prepare hypoimmunogenic mesenchymal stem cells for cell and gene therapy. *Mol Ther*. 2004;9(5):747-756.
51. Suvas S. Role of substance P neuropeptide in inflammation, wound healing, and tissue homeostasis. *J Immunol*. 2017;199(5):1543-1552.
52. Zieglgänsberger W. Substance P and pain chronicity. *Cell Tissue Res*. 2018;96(1-2):49.